Environ. Sci. Technol. **2006**, *40,* 5688−5695

Zinc Coordination to Multiple Ligand Atoms in Organic-Rich Surface Soils

CARMEN ENID MARTÍNEZ,*,† KATYA A. BAZILEVSKAYA,† AND ANTONIO LANZIROTTI‡

Department of Crop and Soil Sciences, The Pennsylvania State University, University Park, Pennsylvania, and Consortium for Advanced Radiation Sources, The University of Chicago and National Synchrotron Light Source, Brookhaven National Laboratory, New York

We report on the solid-phase speciation of naturally occurring Zn in metalliferous organic-matter-rich surface soils. Synchrotron-based studies were used to probe elemental distribution and associations in soil particles (μ-XRF) together with the mineralogy (μ-XRD) and Zn bonding environment (Zn-μ-XANES) at the micrometer-scale level. The average bonding environment of Zn was also probed for bulk soils using XANES. We found the distribution of elements within soil particles to be heterogeneous; however, some elements are consistently co-located. While conventional XRD analyses of whole soils did not identify any Zn mineral phase, synchrotron-based-μ-XRD analyses indicated that sphalerite (ZnS) is present in a particle from a wetland soil (soil labeled G3). Linear combination fit (LCF) analyses of XANES spectra collected for bulk soils (Zn-XANES) and μm-regions (Zn-μ-XANES) within soil particles suggest Zn bonds to oxygen-, nitrogen-, and sulfur-functional groups in these sulfur-, nitrogen-, and zinc-rich organic surface soils. The XANES spectra of all bulk soils and of all μm-regions except for the wetland soil (G3), where ZnS was the most significant constituent, were best fitted by the Zn-arginine reference compound and therefore seems to indicate Zn bonding to nitrogen. Thus, these results provide compelling evidence of the formation of highly covalent Zn-organic bonds in the organic-rich surface soils that were studied. This may explain in part why metal partition coefficients (K_d) are generally higher in organic soils, and why the toxic thresholds for total metal concentrations are higher in organic than in mineral soils.

Introduction

The biogeochemical cycle of metals classified as chalcophiles (i.e., Ag, Cd, Hg, Zn) includes precipitation as metal sulfides and complexation with organic matter. These interactions are potentially important mechanisms of trace element retention in soils and serve as potential sinks and sources of heavy metals. Reactions that might occur under aerobic (oxic) conditions include the oxidation of sulfides and organic matter which may provoke the concomitant release of heavy metals to the solution phase of soils. Total elemental concentrations and pH are parameters frequently used in regression analysis in an attempt to predict the partitioning of elements between the solid and the solution phase of soils (*1*, *2*). As reported for organic horizons of forest soils (*3*), such regression analyses are inconsistent predictors of metal partitioning. Plant uptake studies have also shown an erratic relationship between the concentration of Zn and Cd in maize and canola and total concentration of Zn and Cd in organic soils (*4*). The reactivity or distribution of metals among the various functional groups present in soil organic matter may explain such inconsistent behavior.

Oxygen, P, N, and S functional groups of soil organic matter provide low to high affinity sites that can bind heavy metals. Presumably, sulfur-containing functional groups in soil organic matter are more effective ligands for chalcophilic metals than oxygen-containing functional groups, although the latter are more abundant. Spectroscopic evidence using X-ray absorption spectroscopy (XAS) and electron spin resonance (ESR), for example, indicates that Pb, Cu, Co, Ni, and Zn form inner-sphere complexes with soil humic substances and that these metals coordinate with oxygen ligands (*5*−*7*). Additional bonding environments, particularly for soft and borderline metals, may include inner-sphere complexes with both S- and N-functional groups. In fact, several studies (*4*, *8*−*11*) provide evidence that Hg, CH_3Hg^+, and Cd bind to sulfur-containing functional groups in soils and humic substances. Zinc was found in coordination with reduced forms of inorganic sulfur (as ZnS) in flooded wetland soils (*12*) and aquifer materials (*13*) of relatively low carbon content. It has also been suggested that Zn coordinates with reduced S-containing functional groups of soil humic substances (*6*). More recently, Sarret et al. (*14*) reported a predominance of Zn complexed to organic matter (∼45%) in the surface organic layer of a soil affected by smelting operations. Although most of the Zn was bonded to organic matter, the identification of specific functional groups involved in such bonding was not successful.

Zinc ligation to functional groups other than oxygen has been reported for biomolecules, such as proteins and DNA, and has shown that Zn binds to S and N functional groups in addition to O functional groups. These studies were performed using laboratory-synthesized molecules or biomolecules purified from organisms (*15*−*20*). Even in these presumably "simpler" systems, discrimination between Zn−O and Zn−N bonding has been elusive to direct spectroscopic analyses (e.g., EXAFS and XANES). Clark-Baldwin et al. (*21*), Penner-Hahn (*22*), and Mijovilovich and Meyer-Klaucke (*23*), for example, pointed out the difficulty in assigning Zn−S, Zn−N, or Zn−O ligation in biological systems such as metalloproteins. However, using crystallographic and spectroscopic (XAS, FTIR) approaches, Zn coordination to ligands other than oxygen has been reported. For example, Zn coordination to three O/N at a distance of 2.04 Å and to one S at a distance of 2.31 Å was reported for the protein farnesyltransferase (*16*), while Cohen et al. (*15*) reported Zn in tetrahedral coordination with cysteine and histidine residues in glial cells missing (GCM) proteins. In order to mimic the commonly found motif in hydrolytic Zn enzymes, Gross and Vahrenkamp (*19*) synthesized a N,N,O polydentate ligand (phenyl or methyl substituted bis(2-picolyl)(2-hydroxybenzyl)amine) to represent a histidine and glutamate or aspartate chemical environment. In this system, Zn was found in four-coordination with two nitrogens and one oxygen from the polydentate ligand and with a water (or hydroxyl) ligand from solution. Furthermore, Zn has been

* Corresponding author tel: 814-863-5394; fax: 814-863-7043; e-mail: cem17@psu.edu.

† The Pennsylvania State University.

‡ Consortium for Advanced Radiation Sources, The University of Chicago and National Synchrotron Light Source, Brookhaven National Laboratory.

10.1021/es0608343 CCC: $33.50
Published on Web 08/10/2006

TABLE 1. Elemental Concentrations (g kg^{-1}), Zn/S_{red} Molar Ratios, Exchangeable Zn (mg L^{-1}), and pH of the Soils[a]

soil	C	H	N	P	S	Ca	Fe	Mn	Zn	Cu	Ni	Zn/S_{red}[2]	exchangeable Zn	pH
M1	329.7	68.6	16.2	1.93	7.46	40.72	8.61	0.38	9.20	0.095	0.018	1.65	29.4	5.58
M2	210.0	90.8	10.5	1.46	7.23	37.90	7.63	0.36	15.80	0.117	0.020	2.71	59.1	5.84
M3	394.0	56.4	20.9	2.83	8.35	64.92	9.31	0.34	5.35	0.080	0.016	0.76	6.19	6.20
M4	372.6	54.5	20.9	2.52	6.64	50.44	9.41	0.90	0.23	0.268	0.008	0.08	0.38	5.69
M5	193.6	58.6	10.7	1.78	4.19	38.06	12.46	0.46	0.15	0.154	0.012	0.05	0.12	6.10
M6	424.1	64.9	31.1	1.74	9.54	28.43	14.83	0.16	4.69	0.132	0.023	0.69	30.9	4.52
M7	343.9	75.1	25.2	1.61	8.47	25.77	12.90	0.19	3.58	0.131	0.019	0.70	35.3	4.46
M8	426.6	63.4	29.2	2.05	9.31	26.27	13.02	0.19	2.82	0.112	0.020	0.34	20.4	4.54
M9	387.9	55.4	22.3	1.23	4.76	30.30	20.14	0.48	0.09	0.019	0.018	0.02	0.59	5.19
G1	282.3	40.5	13.5	1.57	3.52	37.77	10.09	0.25	3.20	0.057	0.031	2.82	5.23	6.87
G2	302.6	59.1	14.3	0.73	6.42	34.86	6.64	0.13	3.34	0.062	0.032	0.56	5.66	6.68
G3	278.8	64.4	13.3	0.59	9.07	35.82	4.61	0.09	3.42	0.039	0.028	0.41	4.59	6.70

[a] Some of the data presented in this table (Zn, S, and Zn/S_{red}) was reported previously (*4*). [b] Zn/S_{red} represents the molar ratios of Zn to reduced S as estimated using S-XANES spectroscopy. S_{red} is the fraction of the total S present in the most reduced oxidation state of sulfur (electronic oxidation states ranging from 0.02−0.3). For detailed information see Martínez et al. (*4*).

found in 4- and 6-fold coordination with a combination of N and S functional groups (*20*, *18*), and in 5-fold coordination with N and O functional groups (*17*).

Although most of the current evidence for Zn bonding to organic functional groups other than oxygen comes from biologically relevant systems and have used small molecule analogues, similar functional groups exist in soil organic matter and can potentially bind Zn and other metals. In spite of the difficulty in identifying metal bonding to nitrogen functional groups, several studies report that nitrogen binds to metals in environmental systems. Punshon et al. (*24*), for example, reported similarities between the XANES spectrum of Ni in annual rings of black willow and a Ni-histidine reference compound while Salt et al. (*25*) reported that about 70% of intracellular zinc in roots of the hyperaccumulator *Thlaspi caerulescens* was coordinated with histidine. A XANES study of Cu bonding to humic substances (*26*) has also shown nitrogen involvement at low Cu/C ratios (<0.005).

Our study focuses on the solid-phase speciation of Zn in natural metalliferous organic-rich surface soils. Specifically, we probed the elemental composition, distribution, and associations in soil particles using μ-XRF and identified minerals at microlocations within soil particles using μ-XRD. We also determined the chemical bonding environment of Zn at microsites within soil particles (Zn-μ-XANES) and in bulk soils (Zn-XANES) by analyses of XANES spectra using a linear combination fit (LCF) procedure.

Experimental Section

Soil Samples and Chemical Analyses. Surface soil samples (0−6 cm) were collected from within the Manning peatland region of Western New York (labeled Manning 1−9) and from a wetland near Guelph, Ontario, adjacent to dolomite outcrops (labeled Guelph 1−3). The soils were air-dried and analyzed for total elements using a standard nitric−perchloric acid wet-ash digestion procedure (*27*), and the acid digests were analyzed for metals, calcium, phosphorus, and sulfur by ICP emission spectrometry. Carbon, hydrogen, and nitrogen were determined by combustion (CHN-600 Carbon-Hydrogen-Nitrogen Determination, LECO Corporation). The elemental composition of the soils is presented in Table 1.

An ion exchange reaction was performed by adding 25 mL of a 0.01 M $Ca(NO_3)_2$ solution to a centrifuge tube containing 2.5 g of soil (dry-weight basis). The soil−$Ca(NO_3)_2$ suspension was shaken for 4 h in an end-over-end shaker after which the suspension was centrifuged for 10 min at 15 000 rpm. The supernatant was then filtered using a 0.22 μm membrane filter and the concentration of Zn was measured by atomic absorption (Instrumentation Laboratories Video 22 AA/AE spectrometer). The pH of the 0.01 M $Ca(NO_3)_2$ extract was measured and is reported in Table 1.

Spectroscopic Studies. Synchrotron-based spectroscopic techniques were used to study the distribution and associations of several elements in soil particles, and to obtain molecular level information of the chemical forms of Zn present in microenvironments within soil particles as well as in bulk soils.

Micro-Beam Analyses of Soil Particles. Thin sections of soil particles were prepared using paraffin as the embedding medium (Peel-A-Way Micro-Cut Paraffin melt point 62−64 °C, Gold Standard Series, Polysciences, Inc.). Soil particles were placed on a 2 × 2 cm stainless steel mold and 62 °C paraffin was added to cover the soil particles and fill the mold. The soil particles were soaked in paraffin for 5 h at 62 °C to allow for paraffin penetration into the particles porosity. The molds containing the paraffin and soil particles were dried for 4 h on a 45 °C warming plate. The embedded soil particles were then sectioned to 20 μm thickness with a microtome using a disposable cutting knife. A slide was made in which the thin sections containing the soil particles were placed between two sheets of Mylar film (2.5 μm thick, Chemplex Industries, NY). X-ray micro-beam studies (fluorescence, diffraction, absorption) were performed at Beamline X-26A of the National Synchrotron Light Source (NSLS), Brookhaven National Laboratory (Upton, NY) under standard operating conditions (2.801 GeV and a current ranging from 250 to 100 mA).

Micro-X-ray fluorescence maps (μ-XRF maps) were recorded using a solid-state energy dispersive detector (Canberra SL30165 Si (Li)). The monochromatic beam energy was set at 15 KeV using a Si {111} channel-cut monochromator and the beam was focused to approximately 14 × 10 μm using rhodium-coated Kirkpatrick-Baez focusing optics. Micro-XRF maps were obtained using a 22 μm step size and counts were collected for 50 s per pixel. Although a hard X-ray microprobe designed for elements with atomic number >20, we were able to obtain fluorescence maps for sulfur (K-edge at 2472 eV) because of the high concentration of this element in the soils under investigation (Table 1). Micro regions (14 × 10 μm spots) within soil particles were selected for additional analyses (μ-XRF spectra, μ-XRD, and Zn-μ-XANES) based on the elemental data obtained from μ-XRF maps. Selection of regions for micro-beam analyses was based on the presence, absence, and relative ratios (qualitative only) of elements such as Zn, Ca, Fe, Mn, and S. Energy spectra (μ-XRF spectra) of individual 14 × 10 μm regions were collected for 300 s.

A Bruker SMART 1500 charge-coupled detector (CCD) was used for microcrystallography (μ-XRD) studies and was

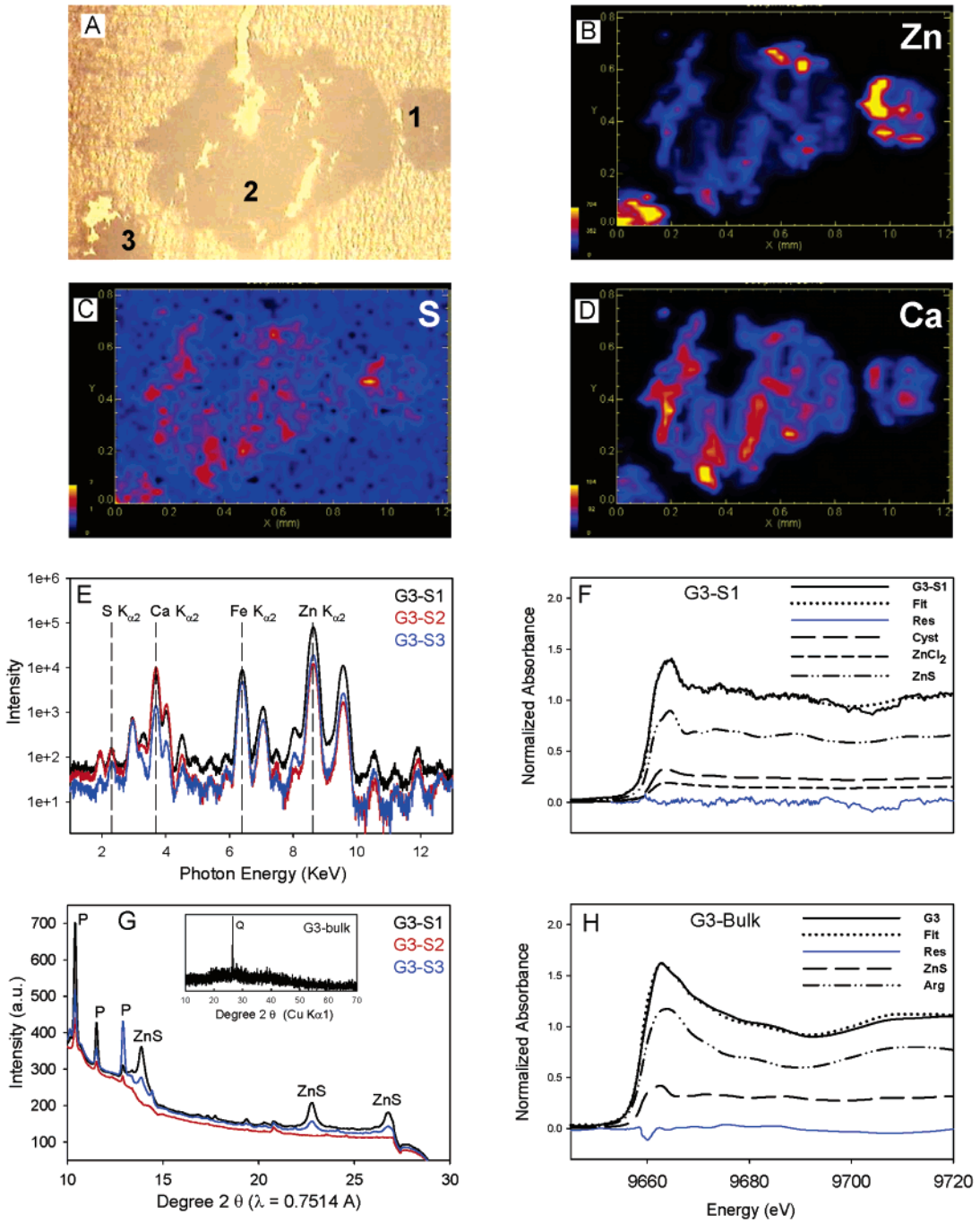

FIGURE 1. Synchrotron-based X-ray analyses for the soil labeled Guelph 3 (G3). Panel A shows a soil particle 1200 × 800 μm in size. Panels B–D show micro-X-ray fluorescence (μ-XRF) maps of Zn, S, and Ca for the soil particle. Panels E and G show, respectively, the μ-XRF spectra and the two-dimensional μ-XRD spectra of three 14 × 10 μm regions within the soil particle (labeled 1, 2, and 3 in Panel A); the XRD pattern of the bulk soil is shown as an insert in Panel G. Results of linear combination fit (LCF) analyses of a 10 × 14 μm region (G3-S1) and the bulk soil (G3-bulk) are presented in panels F and H, respectively.

positioned at approximately 200 mm from the sample. Two-dimensional μ-XRD patterns were collected at the same microregions as the μ-XRF spectra with a wavelength (λ) of 0.75140 or 0.71073 Å. Micro-X-ray diffractograms were collected for 60 s. Two-dimensional diffractograms (2D Debye Scherrer rings) were converted to one-dimensional 2θ scans using the software package Fit2D (Andy Hammersley/ESRF, version V10.132, 2001). The embedding material (paraffin) crystallizes, thus producing peaks in the μ-XRD patterns. The paraffin peaks are labeled with a "P" in the μ-XRD patterns presented in Figures 1 and 2 (also in Figure 1, Supporting Information).

Zinc-XANES (X-ray absorption near edge spectroscopy) spectra were collected on 14 × 10 μm regions (Zn-μ-XANES) of selected areas within soil particles and for Zn standards. The spectra were recorded at the Zn K-edge (9659 eV) in fluorescence mode using a solid-state energy dispersive detector (Canberra SL30165 Si (Li)) positioned 90° to the incident beam. Scans were collected from 100 eV below to 500 eV above the Zn absorption edge. Data reduction and normalization of the original spectra followed standard procedures (*28*). Data reduction and analyses were performed using the computer program Athena (Athena 0.8.041, Bruce Ravel, 2005).

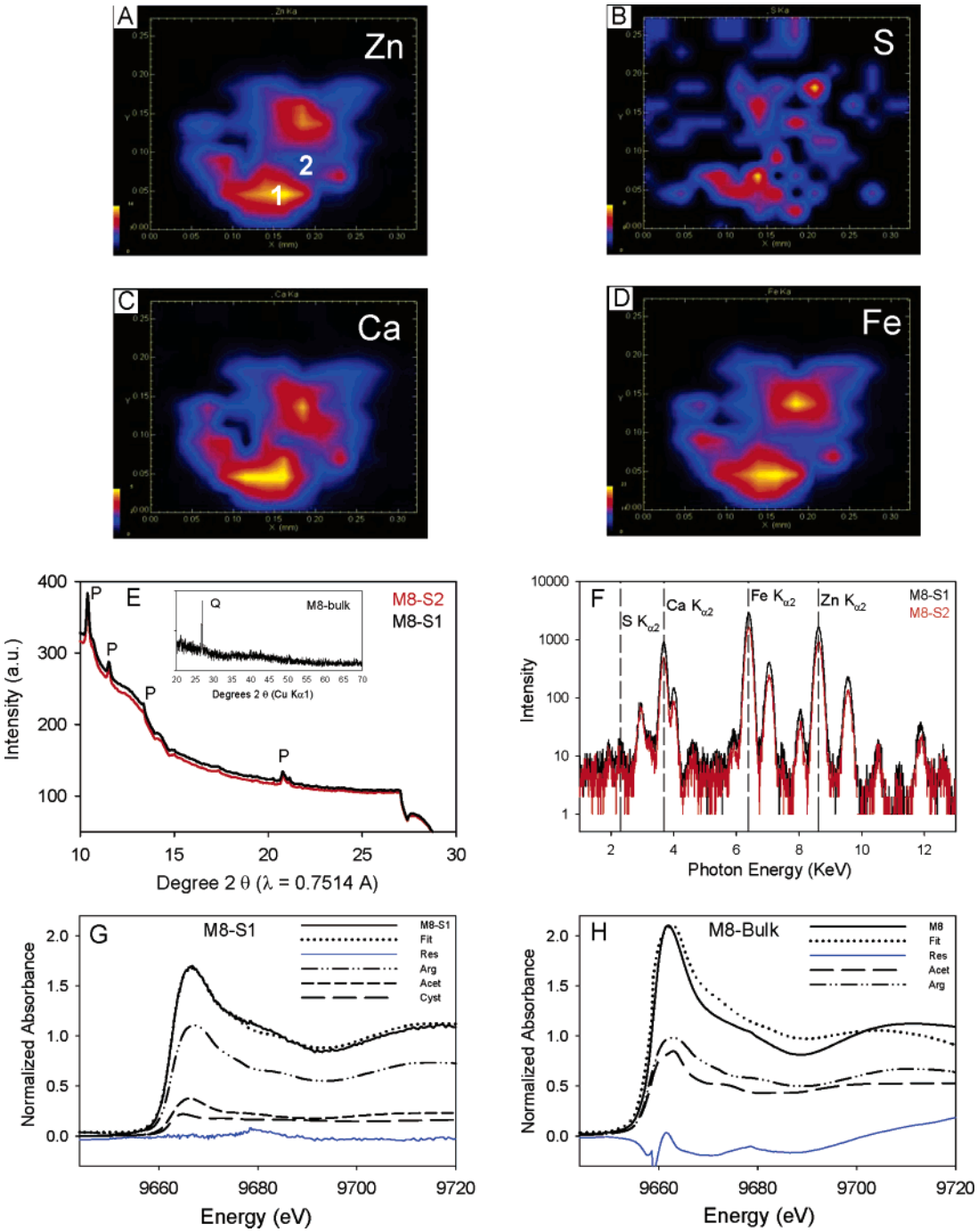

FIGURE 2. Synchrotron-based X-ray analyses for the soil labeled Manning 8 (M8). Panels A−D are micro-X-ray fluorescence (μ-XRF) maps showing the distribution of Zn, S, Ca, and Fe in the soil particle. The two-dimensional μ-XRD patterns (panel E) and the μ-XRF spectra (panel F) of two 14 × 10 μm regions (M8-S1 and M8-S2) are also shown. The XRD of the bulk soil is shown as an insert in panel E. Linear combination fit (LCF) results for a micro-region (M8-S1) and for the bulk soil (M8) are presented in panels G and H, respectively.

The experimental Zn-μ-XANES fluorescence spectra were analyzed using the linear combination fit (LCF) procedure included in the program Athena. In essence, the LCF procedure involves the comparison of XANES spectra collected for a sample with the spectra of model compounds. The LCF procedure yields information on the likely identity of Zn species present in the soils. The XANES spectra of several Zn standards were collected and made available to reconstruct the original soil spectra including (reagent grade powders purchased from Sigma or Alfa Aesar): $ZnCl_2$, Zn−acetate, ZnS, ZnO, $ZnCO_3$, $Zn_3(PO_4)_2$, and $ZnSO_4$. The complexes Zn−cysteine and Zn−arginine were prepared in the laboratory by mixing the ligand and Zn^{2+} at a molar ratio of 10:1 (Zn = 0.01 M) and pH adjustment to 6.5. The standards used in the LCF procedure were selected based on what we know about our system through wet chemical analyses and additional spectroscopic techniques. We also considered the organic forms of nitrogen present in soils since fractionation of soil N using acid hydrolysis shows that amino acid N constitutes from 30−45% of the total soil N and the hydrolyzable unknown N (HUN) fraction (non-α-amino-N of arginine, for example) constitutes 10−20% of the total soil N (*29*). In organic soils, the amino acid N can be as high as ~60% and the HUN fraction can be as high as ~30% (*29*). Moreover, the determination of amino acids in soil acid hydrolysates by paper partition and ion-exchange chroma-

tography has shown that arginine is more abundant in soils than histidine (*29*, *30*). More importantly, studies using circumneutral and acidic fen and peat soils containing from 1.5 to 2.6% N showed that arginine is far more abundant than histidine (*30*). Acetate was chosen to represent the more prevalent and weaker oxygen functional groups of soil organic matter. Citrate was not used because it is not considered representative of soil organic matter functional groups; it is presumably too strong of a ligand for this purpose. Thus, the standards used mimic potential Zn binding sites in soil organic matter and also included zinc sulfide (ZnS).

The experimental Zn-μ-XANES fluorescence spectra were fitted by combining normalized spectra of up to three Zn standards, with a fitting range from −20 to +60 eV relative to the Zn K-edge. The only physical constraints in our LCF procedure were that the weights of the standards should be between 0 and 1 and that a maximum of three standards could be selected. The weights were not forced to sum to one and the energy was fixed. Thus, compliance with the physical constraints and a sum of components (weights) close to one validates our LCF procedure. The goodness of fit is judged by the R-factor (or normalized sum of squares, NSS), the sum of components, and the spectral match between the sum of components (Fit) and experimental spectra (visual inspection).

Zn-XANES Analyses of Bulk Soil. The zinc K-edge (9659 eV) XANES spectra of bulk soils were collected at Beamline X-18B of the National Synchrotron Light Source (NSLS), Brookhaven National Laboratory, under standard operating conditions (2.801 GeV and a current ranging from 250 to 100 mA). A channel cut Si {111} crystal was used as the monochromator. Each soil sample was pressed into a 1.5-mm thick acrylic holder with a Mylar film (2.5 μm thick, Chemplex Industries, NY) window. The spectra were recorded in fluorescence mode using a PIPS (passivated implanted planar silicon) detector positioned 90° to the incident beam. The monochromator was detuned 70% at the Zn K-edge in order to reduce fluorescence induced by high-order harmonics. The Zn K-edge spectrum (assigned a value of 9659 eV) of a Zn metal foil was used for energy calibration. Scans were collected from 150 eV below to 800 eV above the Zn absorption edge. Two to four spectra were recorded for each soil sample, depending on the concentration of Zn. Zn standards were run using the same parameters as for the samples but only 1 or 2 scans were collected. Data reduction of bulk soil Zn-XANES spectra included averaging of 2−4 individual scans and normalization. The experimental Zn-XANES fluorescence spectra of bulk soils were analyzed using the linear combination fit (LCF) procedure as described in the previous section for analyses of Zn-μ-XANES spectra.

Results and Discussion

Elemental Composition and Exchangeable Zn. Zinc concentrations in the organic surface soils range from typical to highly elevated values (Table 1). Elemental analyses also testify to the elevated concentrations of sulfur and nitrogen in the soils. Sulfur concentrations range from 3.52 to 9.54 g S kg^{-1} soil, and nitrogen concentrations range from 10.5 to 31.1 g N kg^{-1} soil (Table 1). A soil is considered S- and N-rich when concentrations exceed 1 and 15 g kg^{-1} of S and N, respectively (*31*). We determined (*4*) the electronic oxidation states of S (using sulfur-XANES analyses) in the soils of this investigation and found that 35−45% of the total soil S exists in the most reduced electronic oxidation states (i.e., sulfides R−S−R and thiols R−S−H) and that 50−70% exists in intermediate electronic oxidation states (i.e., sulfoxide, R−SO−R = 20−38%; and sulfonate, $R-SO_3-H$ = 23−36%). Generally, less than 5% of the total S occurs in the most oxidized forms of sulfur (e.g., sulfate, $R-OSO_3-H$). Furthermore, the Zn/S_{red} molar ratio ranges from 0.02 to 2.71 and the Zn/N molar ratio ranges from 0.0025 to 0.333; these ratios would permit Zn ligation to S- and N-functional groups in these organic soils. The Zn/C molar ratio for most soils falls within the range 0.0001−0.0138, with an average value of 0.003. Although showing a relatively high degree of decomposition (C/N molar ratios from 16 to 25), the soils have a low degree of aromaticity or condensation (C/H molar ratios from 0.2 to 0.6). The degree of aromaticity may reflect on the type of O-, N-, and S-functional groups present in the soils.

The ion exchange experiment using a calcium (Ca) solution to displace exchangeable Zn shows that only a fraction of the total soil Zn is easily exchangeable (Table 1). Salt extractable Zn ranges from 0.80 to 6.5% of the total soil Zn in soils with pH values from 5.2 to 6.9. As expected, the more acid peats (pH 4.5) have a higher percentage (6.6−9.9%) of the total soil Zn in exchangeable forms.

Elemental Distribution and Zn Bonding Environment. Microprobe-X-ray fluorescence (μ-XRF) analyses exposed the elemental distribution and associations within soil particles. Micro-X-ray fluorescence (μ-XRF) maps (Figures 1 and 2) indicate that Zn, Ca, S, and Fe are distributed throughout soil particles; however, the relative concentration of individual elements varies within soil particles and is heterogeneous. The chemical bonding environment of elements such as Zn, for example, may differ in Zn-rich and Zn-poor regions. As shown in Figure 2 (panels A−D and F), Zn-, S-, Ca-, and Fe-rich areas can be co-located; yet, element rich areas are also segregated from one another as illustrated in Figure 1 for Zn and Ca (panels B−E). Our selection of micrometer regions for detail investigations of the mineralogy (μ-XRD) and chemical bonding environment (Zn-μ-XANES) was based on the relative concentration (qualitative only) of key elements (e.g., Zn, S, Ca) as shown by μ-XRF maps and energy spectra.

Conventional XRD analyses of bulk soils as well as synchrotron-based μ-XRD of micro-regions within soil particles (Figures 1 and 2 and Figure 1, Supporting Information) indicate a lack of crystalline mineral phases in most of the organic-rich surface soils under investigation. Conventional XRD also failed to identify a Zn mineral phase in spite of the highly elevated concentrations of Zn. Only quartz, and sometimes dolomite, was detected (inserts in Figure 1, panel G; Figure 2, panel E; and Figure 1, Supporting Information, panel E). Nevertheless, synchrotron-based μ-XRD detected sphalerite (ZnS, d-spacings of 0.3123, 0.1912, and 0.1633 nm) at two microregions within a soil particle from the soil labeled G3 (Figure 1, panel G). This soil does not have the highest concentration of total Zn (Table 1), however, synchrotron-based XRD (for bulk samples) also identified a ZnS mineral phase (figure not shown). The Guelph soils (G series) were collected from a wetland, and although surface soils, they remain flooded for long periods of time. Notice also that many of the Manning soils (M series) with similar Zn/S_{red} molar ratios do not show XRD peaks indicative of ZnS; this is perhaps a consequence of the many years (>60 years) of draining the soils for agricultural purposes. It seems that prevalent redox conditions, perhaps more than elemental concentrations or Zn/S_{red} molar ratios, determine the chemical forms of Zn present in the surface soils under investigation. In a previous study (*4*) a ZnS mineral phase was identified (using EDS) in the soil labeled M2; this ZnS mineral, however, had a blocky morphology (square edges) and may have derived from sphalerite initially present in the outcrop (*32*). Albeit μ-XRD did not detect any crystalline mineral phase in the soils studied (except in soil G3), μ-XRF maps and spectra indicate a close association between Zn and S, thus suggesting that organic S may be involved in the retention of Zn in these soils. It is perhaps possible, although unlikely, that Zn- and S-rich micrometer regions contain conglomerates of nanometer-sized Zn-S spheroids (*33*) and

TABLE 2. Zinc Species Identified by Linear Combination Fit (LCF) Analyses of Bulk and Micrometer Scale Zn-XANES Spectra[a]

soil	$ZnCl_2$ (aq)	Zn−Acetate	Zn−Arginine	Zn−Cysteine	ZnS	sum	R-factor (%)[b]
LCF analyses for Zn-XANES of bulk soils							
M 1		**0.70 (0.14)**	0.36 (0.23)			1.06	0.855
M 2		0.27 (0.03)	**0.69 (0.02)**		0.03 (0.02)	0.99	0.052
M 3		0.40 (0.06)	**0.66 (0.15)**			1.06	0.242
M 7		**0.59 (0.16)**	**0.56 (0.30)**			1.15	1.146
M 8		0.50 (0.08)	**0.59 (0.19)**			1.09	0.416
G 1		0.09 (0.04)	**0.96 (0.26)**			1.05	0.182
G 2		0.10 (0.02)	**0.89 (0.08)**	0.04 (0.01)		1.03	0.057
G 3			**0.71 (0.03)**		0.29 (0.02)	1.00	0.076
LCF analyses for Zn-μXANES of selected micrometer regions							
M1-S1			**0.76 (0.02)**	0.19 (0.07)	0.07 (0.07)	1.02	0.095
M1-S2			**0.78 (0.02)**	0.12 (0.08)	0.12 (0.08)	1.02	0.130
M3-S1	0.27 (0.08)		**0.46 (0.02)**	0.28 (0.08)		1.01	0.159
M3-S2		0.11 (0.04)	**0.75 (0.04)**	0.16 (0.01)		1.02	0.118
M8-S1		0.21 (0.02)	**0.64 (0.03)**	0.15 (0.01)		1.00	0.065
G1-S1			**0.77 (0.01)**	0.23 (0.02)		1.00	0.036
G2-S1			**0.78 (0.01)**	0.22 (0.02)		1.00	0.114
G3-S1	0.14 (0.05)			0.23 (0.08)	**0.62 (0.08)**	0.99	0.073

[a] Zinc species reported as a fraction. Number in parentheses is the variation (1s) in the fraction. [b] R-factor $= \Sigma_i(\text{experimental} - \text{fit})^2/\Sigma_i(\text{experimental})^2$, where the sums are over the data points in the fitting region. R-factors and NSS (normalized sum of squares) are calculated in the same manner.

that such spheroids are invisible to μ-XRD analyses. In fact, using SEM and synchrotron-based XRD and Zn-EXAFS analyses for bulk samples, we found ZnS spherules in deep (45−70 cm depth) organic soils from the same region of Western New York, but not in corresponding organic surface soils (unpublished results).

Linear combination fit (LCF) analyses of Zn-XANES spectra allow us to estimate the relative proportions of Zn species present in the Manning and Guelph soils. Since conventional XRD failed to identify mineral phases other than quartz and dolomite, and μ-XRD detected ZnS in only one of the samples, we determined that it was not appropriate to include inorganic phases except ZnS in our LCF analyses. Specifically, we included $ZnCl_2$, Zn−acetate, Zn−arginine, Zn−cysteine, and ZnS (Table 2). Collectively these species represent outer-sphere Zn^{2+} complexes, Zn complexes with O-, N-, and S-functional groups of organic matter, and an inorganic phase, ZnS. The most striking result from LCF analyses of XANES spectra is the selection of the Zn−arginine complex as the predominant Zn specie present in both bulk soils and micrometer regions within soil particles (Table 2; Figure 1, panel H; Figure 2, panels G, H; Figure 1, Supporting Information, panels B, D, F). An exception to the previous statement is a micrometer region within soil G3, where ZnS was the most significant constituent (Figure 1, panel F); ZnS was also identified by μ-XRD (Figure 1, panel G). Note also that the Zn−cysteine and the Zn−acetate standards were consistently selected in analyses of μm-regions and bulk soils, respectively. Selection of the Zn−cysteine standard is in agreement with μ-XRF maps and spectra showing that Zn and S are co-located. The Zn−acetate standard was not chosen in the soil labeled G3 (bulk) where ∼30% contribution came from ZnS (Figure 1, panel H); the presence of ZnS was confirmed by synchrotron-based XRD of the bulk soil. Although $ZnCl_2$ (representing aqueous Zn^{2+}, an outer-sphere complex) was rarely selected in LCF analyses, a fraction of the total soil Zn (0.80−10%) was desorbed by a $CaCl_2$ solution and is therefore exchangeable (Table 1). At least a portion of the Zn−acetate component should account for outer-sphere Zn complexes. A poor correlation was found, however, between the fraction of the Zn−acetate component in bulk soils and $CaCl_2$ exchangeable Zn (figure not shown). In general, LCF analyses of bulk soils suggest Zn ligation to O- and N-functional groups of organic matter while contributions from O-, N-, and S-functional groups are implied at the μm-scale. Yet, the proportions of Zn species in bulk soils and μm regions differ. Our results are in agreement with the work of Sarret et al. (*14*). Although these authors were not able to identify specific functional groups involved in Zn retention, they reported the combined contribution of organic matter functional groups and outer-sphere Zn-complexes to be ∼65% in an organic layer of a soil known to contain mineral phases (franklinite, sphalerite, willemite). Also, our soils have Zn/C molar ratios within the range 0.0001 to 0.005 (with one soil at 0.0138); these ratios are within the range of Cu/C ratios (<0.005) found by Frenkel et al. (*26*) to be necessary to detect nitrogen involvement in Cu bonding to humic substances.

When we purposely excluded Zn−arginine as a standard, Zn−acetate and $ZnCl_2$ standards were selected by LCF analyses as contributors to the experimental spectra. This resulted in significant increases in the R-factor (∼25% to ∼250% increase relative to the R-factor with Zn−arginine present), and in decreased similarity (visual inspection) between the experimental and fit spectra. A few LCF results were slightly improved by selection of $Zn_3(PO_4)_2$, ZnO, or $ZnCO_3$ instead of a Zn−organic complex, namely, Zn−acetate. The inclusion of inorganic species (all with Zn−O bonding environment) also caused a reduction in the contributions of Zn−arginine and/or Zn−cysteine standards to the experimental spectra. This is most likely influenced by the fact that inorganic mineral species (or standards) generate more intense signals (oscillations) than the light elements present in organic materials and metals in outer-sphere complexes. The spectra of mineral species can therefore mask the contribution from soil organic matter functional groups.

Involvement of nitrogen functional groups in Zn retention is likely since nitrogen is present in relatively high concentrations and the concentration of metals known to bind to N functional groups (i.e., Cu and Ni) is low in the soils under study (Table 1). Furthermore, the stability constants for zinc−ligand complexes (Table 1, Supporting Information) suggest that Zn can bind to S- and N-containing functional groups of soil organic matter in addition to binding to O-containing functional groups. Thermodynamic calculations (*34*) using equilibrium constants for the formation of Zn−organic complexes at a pH of 6.5 indicate that for a 1:1:5:10 Zn/cysteine/arginine/acetate molar ratio (Zn = 0.01 M), ∼42% of the Zn binds to arginine while ∼9% forms acetate species, ∼42% forms cysteine species, and ∼6% exists as the aqueous Zn^{2+} specie (Figure 3). A Zn/cysteine/arginine/acetate molar

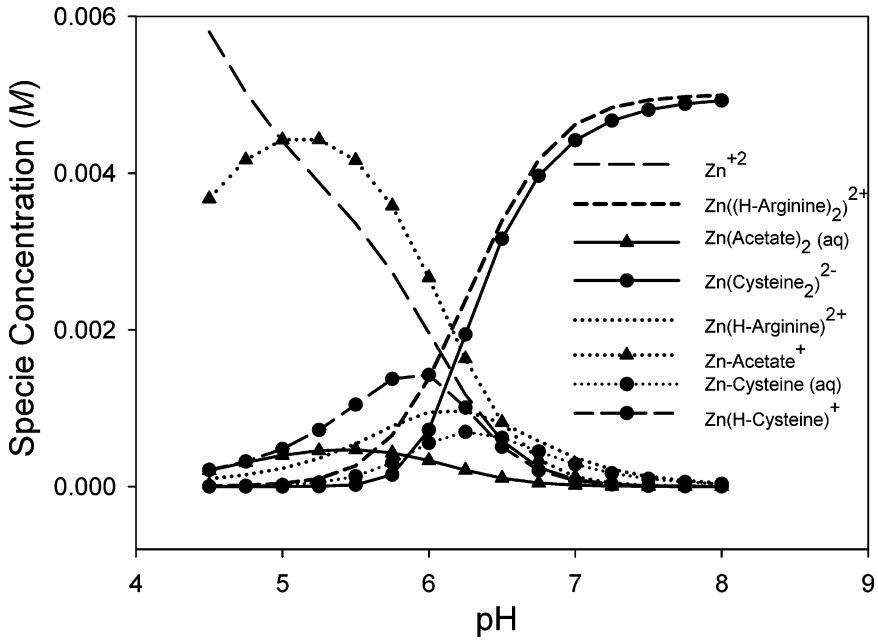

FIGURE 3. Speciation results for the formation of Zn−organic complexes in a 1:1:5:10 Zn/cysteine/arginine/acetate system at pH 6.5.

ratio of 1:1:5:50 (pH 6.5) results in ~30% acetate species, ~26% arginine species, ~38% cysteine species, and ~4% Zn^{2+}. Lowering pH shifts Zn distribution among species, resulting in greater contributions from acetate and aqueous Zn^{2+} species and smaller contributions from arginine and cysteine species. Thermodynamic calculations are in reasonable agreement with our LCF results (Table 2).

Hence, spectroscopic analyses of bulk soils and μm-regions within soil particles suggest Zn bonds to oxygen-, nitrogen-, and sulfur-functional groups in these sulfur-, nitrogen-, and zinc-rich organic surface soils. In organic soils, Zn bioavailability might be determined by the type of complexes Zn forms with organic matter, which depends on the competitive reactivity of different functional groups present in organic materials. The preferential bonding of zinc to N- or S-containing functional groups, which provide higher affinity sites than O-containing functional groups, may explain why organic soils have higher sorption capacity for metals compared to mineral soils.

Acknowledgments

C.E.M. acknowledges funding from the National Science Foundation (award EAR-0311934), which supported this research. K.A.B. is supported by the EMSI program of the NSF (CHE-0431328). C.E.M. thanks Murray B. McBride for providing some of the data presented in Table 1. This research was carried out in part at the National Synchrotron Light Source, Brookhaven National Laboratory, which is supported by the U.S. Department of Energy (DE-AC02-98CH10886). X-ray spectroscopy studies were performed at beamlines X-26A and X-18B of the NSLS. Beamline X-26A is supported by the Division of Geosciences (DE-FG02-92ER14244) and Environmental Remediation Sciences (DE-FC09-96-SR18546) of the Department of Energy.

Supporting Information Available

Table S1 presents the stability constants for Zn, Cu, and Ni with ligands containing O-, N-, and S-functional groups. Figure S1 shows synchrotron-based X-ray analyses for the soil labeled Manning 3 (M3). This material is available free of charge via the Internet at http://pubs.acs.org.

Literature Cited

(1) Jopony, M.; Young, S. D. The solid-solution equilibria of lead and cadmium in polluted soils. *European J. Soil Sci.* **1994**, *45*, 59−70.

(2) McBride, M. B.; Sauvé, S.; Hendershot, W. Solubility control of Cu, Zn, Cd and Pb in contaminated soils. *European J. Soil Sci.* **1997**, *48*, 337−346.

(3) Sauvé, S.; Manna, S.; Turmel, M.-C.; Roy, A. G.; Courchesne, F. Solid-solution partitioning of Cd, Cu, Ni, Pb, and Zn in the organic horizons of a forest soil. *Environ. Sci. Technol.* **2003**, *37*, 5191−5196.

(4) Martínez, C. E.; McBride, M. B.; Kandianis, M. T.; Duxbury, J. M.; Yoon, S.; Bleam, W. F. Zinc−sulfur and cadmium−sulfur association in metalliferous peats: evidence from spectroscopy, distribution coefficients, and phytoavailability. *Environ. Sci. Technol.* **2002**, *36*, 3683−3689.

(5) Xia, K.; Bleam, W.; Helmke, P. A. Studies of the nature of Cu^{2+} and Pb^{2+} binding sites in soil humic substances using x-ray absorption spectroscopy. *Geochim. Cosmochim. Acta* **1997**, *61*, 2211−2221.

(6) Xia, K.; Bleam, W.; Helmke, P. A. Studies of the nature of binding sites of first row transition elements bound to aquatic and soil humic substances using x-ray absorption spectroscopy. *Geochim. Cosmochim. Acta.* **1997**, *61*, 2223−2235.

(7) McBride, M. B. Transition metal bonding in humic acid: An ESR study. *Soil Sci.* **1978**, *126*, 200−209.

(8) Skyllberg, U. L.; Xia, K.; Bloom, P. R.; Nater, E. A.; Bleam, W. F. Binding of Hg (II) to reduced sulfur in soil organic matter along upland-peat soil transects. *J. Environ. Qual.* **2000**, *29*, 855−865.

(9) Hesterberg, D.; Chou, J. W.; Hutchison, K. J.; Sayers, D. E. Bonding of Hg(II) to reduced organic sulfur in humic acid as affected by S/Hg ratio. *Environ. Sci. Technol.* **2001**, *35*, 2741−2745.

(10) Yoon, S.-J.; Diener, L. M.; Bloom, P. R.; Nater, E. A.; Bleam, W. F. X-ray absorption studies of CH_3Hg^+-binding sites in humic substances. *Geochim. Cosmochim. Acta.* **2005**, *5*, 1111−1121.

(11) Karlsson, T.; Persson, P.; Skyllberg, U. Extended X-ray absorption fine structure spectroscopy evidence for the complexation of cadmium by reduced sulfur groups in natural organic matter. *Environ. Sci. Technol.* **2005**, *39*, 3048−3055.

(12) Bostick, B. C.; Hansel, C. M.; La Force, M. J.; Fendorf, S. Seasonal fluctuations in zinc speciation within a contaminated wetland. *Environ. Sci. Technol.* **2001**, *35*, 3823−3829.

(13) Hesterberg, D.; Sayers, D. E.; Zhou, W. Q.; Plummer, G. M.; Robarge, W. P. X-ray absorption spectroscopy of lead and zinc speciation in a contaminated groundwater aquifer. *Environ. Sci. Technol.* **1997**, *31*, 2840−2846.

(14) Sarret, G.; Balesdent, J.; Bouziri, L.; Garnier, J.; Marcus, M. A.; Geoffroy, N.; Panfill, F.; Manceau, A. Zn speciation in the organic horizon of a contaminated soil by micro-X-ray fluorescence,

micro- and powder-EXAFS spectroscopy, and isotopic dilution. *Environ. Sci. Technol.* **2004**, *38*, 2792−2801.
(15) Cohen, S. X.; Moulina, M.; Schilling, O.; Meyer-Klaucke, W.; Schreiber, J. Wegner, M.; Müller, C.W. The GCM domain is a Zn-coordinating DNA-binding domain. *FEBS Lett.* **2002**, *528*, 95−100.
(16) Tobin, D. A.; Pickett, J. S.; Hartman, H. L.; Fierke, C. A.; Penner-Hahn, J. E. Structural characterization of the zinc site in protein farnesyltransferase. *J. Am. Chem. Soc.* **2003**, *125*, 9962−9969.
(17) Novokmet, S.; Heinemann, F. W.; Zahl, A.; Alsfasser, R. Aromatic interactions in unusual backbone nitrogen-coordinated zinc peptide complexes: A crystallographic and spectroscopic study. *Inorg. Chem.* **2005**, *44*, 4796−4805.
(18) Berry, S. M.; Bebout, D. C.; Butcher, R. J. Solid-state and solution-state coordination chemistry of the zinc triad with the mixed N, S donor ligand bis(2-methylpyridyl) sulfide. *Inorg. Chem.* **2005**, *44*, 27−39.
(19) Gross, F.; Vahrenkamp, H. Zinc complex chemistry of N,N,O ligands providing a hydrophobic cavity. *Inorg. Chem.* **2005**, *44*, 3321−3329.
(20) Reddy, P. R.; Radhika, M.; Manjula, P. Synthesis and characterization of mixed ligand complexes of Zn(II) and Co(II) with amino acids: Relevance to zinc binding sites in zinc fingers. *J. Chem. Sci.* **2005**, *117*, 239−246.
(21) Clark-Baldwin, K.; Tierney, D. L.; Govindaswamy, N.; Gruff, E. S.; Kim, C.; Berg, J.; Koch, S. A.; Penner-Hahn, J. E. The limitations of X-ray absorption spectroscopy for determining the structure of zinc sites in proteins. When is a tetrathiolate not a tetrathiolate? *J. Am. Chem. Soc.* **1998**, *120*, 8401−8409.
(22) Penner Hahn, J. E. Characterization of "spectroscopically quiet" metals in biology. *Coord. Chem. Rev.* **2005**, *249* (1−2), 161−177.
(23) Mijovilovich, A.; Meyer-Klaucke, W. Simulating the XANES of metalloenzymes − a case study. *J. Synchrotron Radiat.* **2003**, *10*, 64−68.
(24) Punshon, T.; Lanzirotti, A.; Harper, S.; Bertsch, P. M.; Burger, J. Distribution and speciation of metals in annual rings of black willow. *J. Environ. Qual.* **2005**, *34*, 1165−1173.
(25) Salt, D. E.; Prince, R. C.; Baker, A. J. M.; Raskin, I.; Pickering, I. J. Zinc ligands in the metal hyperaccumulator *Thlaspi caerulescens* as determined using X-ray absorption spectroscopy. *Environ. Sci. Technol.* **1999**, *33*, 713−717.
(26) Frenkel, A. I.; Korshin, G. V.; Ankudinov, A. L. XANES study of Cu^{2+}-binding sites in aquatic humic substances. *Environ. Sci. Technol.* **2000**, *34*, 2138−2142.
(27) Greweling, T. C. Bull.−N. Y., Agric. Exp. Stn. (Ithaca) **1976**, *6*, 35.
(28) Sayers, D. E.; Bunker G. EXAFS data analysis. In *X-ray Absorption: Principles, Applications, Techniques of EXAFS, SEXAFS and XANES*; Koningsberger, D.C., Prins, R., Eds.; John Wiley & Sons, Inc.: New York, 1988.
(29) Stevenson, F. J. *Humus Chemistry. Genesis, Composition, Reactions*, second edition; John Wiley & Sons, Inc.: New York, 1994.
(30) Bremner, J. M. The amino acid composition of the protein material in soil. *Biochem. J.* **1950**, *47*, 538−542.
(31) Stevenson, F. J.; Cole, M. A. *Cycles of Soil: Carbon, Nitrogen, Phosphorus, Sulfur, Micronutrients*, second edition; John Wiley & Sons, Inc.: New York, 1999.
(32) Cannon, H. L. *Geochemical relations of zinc-bearing peat to the Lockport dolomite, Orleans County, New York;* U.S. Geological Survey Bulletin 1000-D; 1995, pp 119−185.
(33) Moreau, J. W.; Webb, R. I.; Banfield, J. F. Ultrastructure, aggregation-state, and crystal growth of biogenic nanocrystalline sphalerite and wurtzite. *Am. Mineral.* **2004**, *89*, 950−960.
(34) Gustafsson, J. P. Visual MINTEQ, version 2.40; KTH, Department of Land and Water Resource Engineering: Stockholm, Sweden, 2006.

Received for review April 6, 2006. Revised manuscript received July 6, 2006. Accepted July 12, 2006.

ES0608343